

# Journal of Photonics for Energy

PhotonicsforEnergy.SPIEDigitalLibrary.org

## **Review of recent progress in unassisted photoelectrochemical water splitting: from material modification to configuration design**

Piangjai Peerakiatkhajohn  
Jung-Ho Yun  
Songcan Wang  
Lianzhou Wang

**SPIE.**

Piangjai Peerakiatkhajohn, Jung-Ho Yun, Songcan Wang, Lianzhou Wang, "Review of recent progress in unassisted photoelectrochemical water splitting: from material modification to configuration design," *J. Photon. Energy* 7(1), 012006 (2016), doi: 10.1117/1.JPE.7.012006.

# Review of recent progress in unassisted photoelectrochemical water splitting: from material modification to configuration design

Piangjai Peerakiatkhajohn, Jung-Ho Yun, Songcan Wang, and Lianzhou Wang\*

University of Queensland, Nanomaterials Centre, School of Chemical Engineering and AIBN, St. Lucia, Queensland 4072, Australia

**Abstract.** Photoelectrochemical (PEC) energy conversion systems have been considered as a highly potential strategy for clean solar fuel production, simultaneously addressing the energy and environment challenges we are facing. Tremendous research efforts have been made to design and develop feasible unassisted PEC systems that can efficiently split water into hydrogen ( $H_2$ ) and oxygen with only the energy input of sunlight. A fundamental understanding of the concepts involved in PEC water splitting and energy conversion efficiency enhancement for solar fuel production is important for better system design. This review gives a concise overview of the unassisted PEC devices with some state-of-the-art progress toward efficient PEC devices for future sustainable solar energy utilization. © 2016 Society of Photo-Optical Instrumentation Engineers (SPIE) [DOI: [10.1117/1.JPE.7.012006](https://doi.org/10.1117/1.JPE.7.012006)]

**Keywords:** unassisted photoelectrochemical water splitting; hydrogen production; semiconductors; nanostructure engineering; surface modification; tandem configuration.

Paper 16064SS received May 31, 2016; accepted for publication Aug. 8, 2016; published online Aug. 24, 2016.

## 1 Introduction

With the increasing energy consumption and the depletion of fossil fuels, it is urgent to develop clean, earth-abundant, and renewable energy resources to effectively address energy issues. Photoelectrochemical (PEC) water splitting has been found to be a promising approach for directly converting solar energy into sustainable and environmentally friendly hydrogen fuel.<sup>1–5</sup> Over the past four decades, even though great achievements have been obtained, the solar-to-hydrogen (STH) efficiency is still too low for practical applications.<sup>6</sup> The key challenge for efficient solar hydrogen generation is to explore suitable photoelectrode materials that meet the following criteria: (1) broad range of solar spectrum absorption, (2) high photochemical stability, (3) efficient use of photogenerated electrons and holes, (4) suitable band edge positions, (5) low overpotential, and (6) low cost.<sup>7–10</sup> Typically, a single semiconductor is difficult for achieving all of the above requirements. For example,  $TiO_2$  is stable in aqueous electrolytes under light illumination, but its large bandgap (3.0 eV) limits its light utilization to the UV region that accounts for only ~4% of the solar energy on earth, resulting in low STH efficiency.<sup>11,12</sup> On the other hand, although multijunction silicon or heterojunction III–V semiconductors as photoelectrodes considerably increase the visible light conversion efficiency, they increase the cost while shortening the lifetime of the whole devices due to their photocorrosion in aqueous electrolytes.<sup>13–15</sup> Therefore, the number of reliable and reproducible semiconductors for solar water splitting is limited. Combining the advantages of different semiconductors to form heterojunction systems or integrating state-of-the-art semiconductors with photovoltaic (PV) devices to form tandem cells may open up more opportunities, which have been extensively investigated during the past decade.<sup>16–20</sup> Especially, self-driven monolithic and PEC tandem

---

\*Address all correspondence to: Lianzhou Wang, E-mail: [l.wang@uq.edu.au](mailto:l.wang@uq.edu.au)

systems have attracted great attention due to the low cost when compared to the use of only PV devices for water splitting.<sup>21–26</sup> Nevertheless, the obtained STH and stability for the reported systems are still too low for the 10% target toward practical applications, even though many unique and novel material configurations have been revealed in recent years.<sup>27–33</sup>

In this review, we concisely summarize the recent progress and challenges in the unassisted PEC water splitting system, which has been considered as the ultimate solar water splitting process, compared to many reported PEC systems, which still rely on the applied external bias. We pay particular attention to nanostructure engineering of the photoelectrodes and the concepts of PEC configuration design for efficient water splitting. The review will start with some basic principles of unassisted PEC water splitting, followed by the design of photoelectrode materials based on nanostructure engineering and surface modifications. Then, the recent progress of PEC system configurations will be summarized. Finally, a brief overview including the challenges and perspectives of this research field will be given. We believe that this comprehensive review would not only provide important information about the recent progress of unassisted PEC water splitting systems but also could inspire readers to apply the discussed strategies to further improve the PEC solar fuel production performance.

## 2 Principles of Unassisted Photoelectrochemical Systems

Figure 1(a) presents the basic principle of a conventional PEC water splitting system. Under light illumination, electrons ( $e^-$ ) will be excited from the valence band (VB) to the conduction band (CB), where holes ( $h^+$ ) are left in the VB of the working electrode. Then, the electrons transport to the counter electrode and participate in the hydrogen-evolution half-reaction (HER). Meanwhile the holes transfer to the surface of the working electrode and are involved in the oxygen-evolution half-reaction (OER).<sup>34,35</sup> Typically, overall water splitting can be achieved by applying an external bias if the semiconductor itself in the working electrode is suitable only for OER or HER. For example, some metal oxides, such as  $Fe_2O_3$ ,  $WO_3$ , and  $BiVO_4$ , can be used as working electrodes for water splitting with a proper bias, even though their CB positions are unable to reduce water themselves.<sup>36–40</sup>

According to the general mechanism in PEC  $H_2$  production, the selection of light absorbers and device configurations is important in driving effective water splitting reactions. A Z-scheme concept has been developed through a two-step excitation mechanism induced by coupling two different light absorbers, which is inspired by natural photosynthesis in green plants.<sup>41–44</sup> The charge transfer in a Z-scheme system is different from that in the general p-n heterojunction configuration. For p-n heterojunctions, photogenerated electrons in photosystem II (PS II) with higher CB are transferred to photosystem I (PS I) with lower CB to be involved in HER, while holes are transferred to the opposite direction for OER due to the built-in electrical potential in the interfaces [Fig. 1(b)]. By contrast, photogenerated holes in the VB of PS I are promoted in OER, while electrons in the CB of PS II are used for HER in the Z-scheme configuration [Fig. 1(c)]. Thus, the Z-scheme system demonstrates the strong oxidized ability of PS I and the strong reduced ability of PS II. The advantage of the Z-scheme water splitting system is to utilize a wider range of visible light because the energy required to activate each photocatalyst can be reduced as compared to the one-step water splitting system.<sup>45–47</sup> Successful overall water

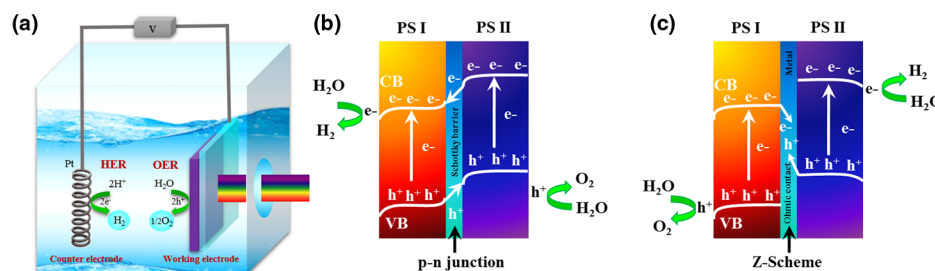


**Fig. 1** (a) A schematic illustration of the photoelectrochemical water splitting process, charge transfer in a heterojunction PEC system with (b) p-n junction type, and (c) Z-scheme configuration.

splitting via two-step photoexcitation under visible light illumination has been reported by combining several semiconductors.<sup>48–51</sup> Especially, the artificial photosynthesis (AP) concept has emerged as an attractive approach to mimic the natural photosynthesis process by utilizing suitable semiconductors to efficiently drive the thermodynamically uphill water splitting reaction under sunlight illumination.<sup>52–55</sup>

### 3 Recent Progress and Challenges of Unassisted Photoelectrochemical Devices

In this section, recent efforts on the development of novel nanostructured design concepts and surface modification strategies for an unassisted PEC water splitting system will be briefly presented and discussed in terms of the improvement of performance.

#### 3.1 Nanostructured Semiconductor Design

In general, PEC performance of the devices depends on the efficient light utilization, photogenerated carrier transport/separation, and stability in the PEC system. Nanostructured semiconductors have been revealed to be promising for PEC water splitting due to their large surface area and size-dependent properties (e.g., tuned bandgap energy, shortened carrier collection pathways, and efficient charge transfer).<sup>56</sup> Therefore, the selection of a suitable semiconductor with excellent nanoarchitecture is of importance for PEC system construction. n-type semiconductors (e.g.,  $\text{WO}_3$ ,  $\text{Fe}_2\text{O}_3$ ,  $\text{TiO}_2$ , and  $\text{BiVO}_4$ ) are commonly developed as photoanodes or top absorbers in tandem devices due to their low VB energy positions with more positive VB potential for water oxidation reaction.<sup>57–61</sup> However, when these semiconductors are used as photoelectrodes, the randomly oriented bulk nanoparticles (NPs) in photoelectrodes might decrease the PEC performance with a high charge recombination rate due to a large number of charge trap sites. To overcome this issue, well oriented one-dimensional (1-D),<sup>62–68</sup> two-dimensional (2-D),<sup>69–73</sup> and three-dimensional (3-D)<sup>74–76</sup> nanostructures have been developed in recent years. The 1-D nanostructures including nanowires,<sup>77–79</sup> nanorods,<sup>80–82</sup> and nanotubes<sup>83–86</sup> provide both efficient light harvesting and superior charge transport for PEC water splitting. Meanwhile, 2-D nanostructures have also shown interesting properties in various photochemical fields.<sup>87–89</sup> In particular, metal oxide and chalcogenide 2-D nanosheets are unique nanostructures with high-specific surface area and excellent crystallinity, which is beneficial for efficient charge separation and migration in water splitting.<sup>90–94</sup> More recently, researchers have integrated different functional materials of 1-D or 2-D structures to construct 3-D hierarchical nanostructures in order to increase large surface areas for light harvesting without inhibiting charge transfer and separation.<sup>95–99</sup> Hence, it is a promising nanostructure model for efficient water splitting due to broader light absorption, rapid charge migration and separation.

On the other hand, p-type semiconductors such as boron-doped Si,<sup>100</sup>  $\text{Cu}_2\text{O}$ ,<sup>101</sup>  $\text{CuInS}_2$ ,<sup>102</sup> and  $\text{GaInP}_2$ <sup>14</sup> exhibit small bandgaps, thereby a significant proportion of visible light can be harvested. However, when p-type materials are employed to PEC water splitting, severe challenges such as large overpotential, instability, and low absorption coefficient have been observed.<sup>103</sup> Thus, recent strategies have been focused on improving the photostability through loading suitable protective layers or coupling with n-type semiconductors to form heterojunctions.<sup>104</sup> For example, n- $\text{TiO}_2$  has been reported as an effective protective layer for enhancing the photostability and photoactivity of p-type photoelectrodes.<sup>105–107</sup> Such a heterojunction concept by coupling different photoanode and photocathode layers would be a promising approach for unassisted PEC water splitting systems. For designing such systems, the nanostructured morphology and crystallinity of semiconductors with suitable CB and VB positions for water splitting and the interfacial properties in the heterojunction should be carefully considered. Moreover, the fabrication process of the photoelectrodes in a PEC system should be optimized by exploring simple, cost-effective, and environmentally friendly techniques. Figure 2 represents the engineering strategies that are critical to meet all requirements for efficient PEC water splitting. The recent reported PEC systems, which have been developed based on these strategies, will be further presented and discussed in Sec. 3.3.

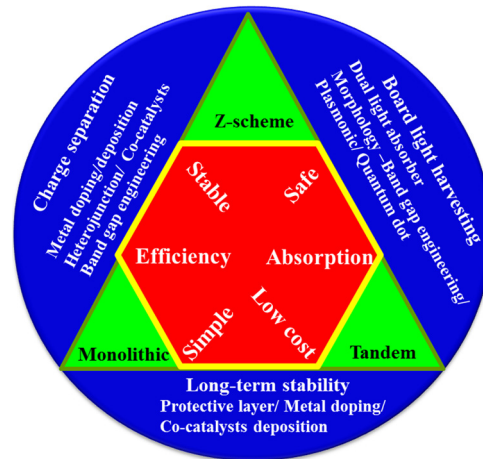


**Fig. 2** The important engineering strategies to achieve efficient PEC water splitting.

### 3.2 Surface Modification of Photoelectrodes

In addition to nanostructure engineering, the surface modification of photoelectrodes is also important for achieving high PEC performance. As the surfaces of the photoelectrode materials are active sites for redox reaction, the surface states are closely related to photon energy absorption properties and surface charge transfer ability of the semiconductors. Doping is one common strategy to improve the conductivity of semiconductors and extend the lifetime of charge carriers by reducing recombination of the photogenerated electron–hole pairs.<sup>108–116</sup> In addition, loading HER or OER cocatalysts on the surface of the semiconductor is also an efficient approach to reduce the charge recombination at a lower applied potential and increase the charge transfer for the water splitting process.<sup>117</sup> Cocatalysts should be optimized to offer highly active sites to separate the photogenerated charges for HER or OER half reactions, avoiding the photogenerated electrons and holes with high redox ability to react with the semiconductor itself, which improves the stability. Noble metals (e.g., Pt) and noble metal oxides (e.g., IrO<sub>2</sub>, RuO<sub>2</sub>) are usually used as effective HER and OER cocatalysts, respectively.<sup>118,119</sup> Nevertheless, it is not favorable to scale up their utilization in PEC devices due to their cost and rarity. Thus, noble metal-free cocatalysts, such as cobalt compounds,<sup>120–126</sup> nickel-based materials,<sup>127,128</sup> and chalcogenides<sup>129–132</sup> for photoelectrode surface modification, have been developed.

In addition, plasmonic NP coupling is another strategy to utilize the optical properties of nanometals for better light harvesting.<sup>133–135</sup> Typically, plasmonic metal NPs can be employed to capture light and transfer the excitation energy through the localized surface plasmon to a combined semiconductor with large bandgap. In general, when plasmonic metal nanostructures are contacted with semiconductors, they should be able to alleviate charge recombination and enhance light absorption, resulting in higher PEC performance than their pure semiconductor counterparts.<sup>136–146</sup> For instance, Zhang et al.<sup>97</sup> studied PEC performance of Au NPs deposited on the TiO<sub>2</sub> bilayered structure photoanode and reported a STH efficiency of 0.71% achieved, around which is one of the highest values reported in Au/TiO<sub>2</sub>-based photoanodes. The excellent PEC water splitting activity in visible light can be ascribed to the generated energetic hot e<sup>-</sup>/h<sup>+</sup> of Au NPs that were injected into the CB of TiO<sub>2</sub> through the excitation and decay of surface plasmons. In another study, the utilization of a plasmonic Au nanohole array combined with Fe<sub>2</sub>O<sub>3</sub> nanorod array photoanode led to significant enhancement of the photocurrent density<sup>147</sup> and a plasmon-induced resonant energy transfer (PIRET) effect was proposed to explain this phenomenon. In addition to photoanodes, CuO nanowires decorated with Ag NPs as photocathodes were also studied in which the surface plasmon energy transfer from Ag NPs contributed to enhanced photocurrent with a STH efficiency of 2.16% achieved.<sup>148</sup> The use of plasmonic Ag NPs deposited on TiO<sub>2</sub> photoanodes can also further improve the photocurrent density by LSPR property of Ag NPs.<sup>149,150</sup>

Recent works on nanostructure engineering and surface modification for innovative PEC system design are summarized in Table 1. It is apparent that many efforts have focused on

**Table 1** PEC devices for solar water splitting.

Photoelectrode system	Cocatalysts	Photocurrent (mA cm <sup>-2</sup> )	Light source	STH/IPCE (%)	References
p-GaInP <sub>2</sub> (Pt)/TJ/GaAs	Pt	120 at ~0.15 V	11 suns, 1.19 ± 0.05 W cm <sup>-2</sup>	STH = 12.4%	Ref. 24
3jn-a-Si	OER: Co-Bi, HER: NiMoZn	~3 at 0 V <sub>RHE</sub>	1 sun, AM 1.5 G	STH = 2.5% (wireless) and 4.7% (wired)	Ref. 151
Si pillars	Mo <sub>3</sub> S <sub>4</sub>	~9 at 0 V <sub>RHE</sub>	λ > 620 nm, 28.3 mW cm <sup>-2</sup>	STH = 10%	Ref. 130
p-Si/SiO <sub>2</sub> /Ti	Pt	~20 at 0 V <sub>RHE</sub>	1 sun, AM 1.5 G	STH = 2.9%	Ref. 152
n + p-Si/TiO <sub>2</sub>	Pt	~22 at 0.3 V <sub>RHE</sub>	λ > 635 nm, AM 1.5 G	IPCE = ~90%	Ref. 153
AlGaAs/Si	RuO <sub>2</sub> /Pt black	20.1, unassisted	135 mW cm <sup>-2</sup>	STH = 18.3%	Ref. 154
W-doped BiVO <sub>4</sub> /Si	Co-Pi	4 at 1.23 V <sub>RHE</sub>	1 sun, AM 1.5 G	STH = 4.9%	Ref. 155
BiVO <sub>4</sub> on 1D ZnO nanorods	Co-Pi	3 at 1.2 V <sub>RHE</sub>	λ > 420 nm, AM 1.5 G	STH = 0.88%	Ref. 68
Ba-Ta <sub>3</sub> N <sub>5</sub> nanorod	IrO <sub>2</sub>	6.7 at 1.23 V <sub>RHE</sub>	1 sun, AM 1.5 G	STH = 1.5%	Ref. 156
WSe <sub>2</sub>	Pt/Ru	15 at 0 V <sub>RHE</sub>	100 mW cm <sup>-2</sup>	η <sub>c</sub> = 7.0%	Ref. 157
Si/TiO <sub>2</sub> nanotree	HER: Pt OER: IrO <sub>x</sub>	—	150 mW cm <sup>-2</sup>	STH = 0.12%	Ref. 79
p-Si/Fe <sub>2</sub> O <sub>3</sub> -AuNPs	Au	2.6 at 0 V <sub>Pt</sub>	60 mW cm <sup>-2</sup>	STH = 6%	Ref. 158
DSSC/WO <sub>3</sub> (n)	Pt	~1.56 at 0 V <sub>RHE</sub>	100 mW cm <sup>-2</sup>	STH = 1.9%	Ref. 22
WO <sub>3</sub> /C <sub>3</sub> N <sub>4</sub>	CoO <sub>x</sub>	5.76 at 2.1 V <sub>RHE</sub>	AM 1.5 G	IPCE = 37.5% at 400 nm and 1.6 V <sub>RHE</sub>	Ref. 95
Pt-doped Fe <sub>2</sub> O <sub>3</sub>	Co-Pi	4.32 at 1.23 V <sub>RHE</sub>	1 sun, AM 1.5 G	IPCE = 50% at 400 nm and 1.23 V <sub>RHE</sub>	Ref. 159
Cu <sub>2</sub> O/(ZnO, Al <sub>2</sub> O <sub>3</sub> )/TiO <sub>2</sub>	Pt	-7.6 at 0 V <sub>RHE</sub>	AM 1.5 G	IPCE = 40% between 350 and 480 nm, 0 V <sub>RHE</sub>	Ref. 160
Cu <sub>2</sub> O/(ZnO, Al <sub>2</sub> O <sub>3</sub> )/TiO <sub>2</sub>	MoS <sub>2+x</sub>	-5.7 at 0 V <sub>RHE</sub>	AM 1.5 G	STH = 7%	Ref. 131
Cu <sub>2</sub> O/BiVO <sub>4</sub>	HER: RuO <sub>x</sub> OER: Co-Pi	1, unassisted	100 mW cm <sup>-2</sup>	STH = 0.5%	Ref. 161
Au at TiO <sub>2</sub> /Al <sub>2</sub> O <sub>3</sub> /Cu <sub>2</sub> O	—	-4.34 at 0 V <sub>RHE</sub>	AM 1.5 G	IPCE = 78% at 340 nm	Ref. 43
C/Cu <sub>2</sub> O/Cu	—	-3.95 at 0 V <sub>RHE</sub>	AM 1.5 G	STH = 0.56% at 0.21 V <sub>RHE</sub>	Ref. 162
CdS/CuGaSe <sub>2</sub>	Pt	~19 at 0 V <sub>RHE</sub>	300 W Xe lamp	STH = 0.83% at 0.2 V <sub>RHE</sub>	Ref. 163
CdS/Ag <sub>x</sub> Cu <sub>1-x</sub> GaSe <sub>2</sub>	Pt	8.1 at 0 V <sub>RHE</sub>	AM 1.5 G	IPCE ≈ 50% at 500 nm and 0 V <sub>RHE</sub>	Ref. 164



**Table 1** (Continued).

Photoelectrode system	Cocatalysts	Photocurrent (mA cm <sup>-2</sup> )	Light source	STH/IPCE (%)	References
CH <sub>3</sub> NH <sub>3</sub> PbI <sub>3</sub> with NiFe DLH/Ni foam	NiFe DLH	10, unassisted	AM 1.5 G	STH = 12.3%	Ref. 165
CH <sub>3</sub> NH <sub>3</sub> PbI <sub>3</sub>	Ni	12 at 0 V <sub>Ag/AgCl</sub>	1 sun, AM 1.5 G	—	Ref. 166

controlling nanostructures, doping with suitable elements, and loading cocatalysts in heterojunction photoelectrodes. However, the high photocurrent and STH efficiency achievements in most of the systems are limited and external bias is generally required for overall water splitting. Notably, multilayered PEC devices composed of nanostructured metal oxide semiconductors, perovskite solar cells (PSCs), and Si photoelectrodes can exhibit high STH up to 10%, whereas such PEC devices are expensive, complicated, and unstable in aqueous electrolyte under light illumination. In order to overcome these drawbacks, the selection of excellent crystalline photoelectrode materials and suitable electrolytes is essentially important, and the overall PEC system should be considered by designing the configuration of multilayered photoelectrodes with protective layers. Such conditions would be the key factors in developing unassisted PEC systems for overall water splitting.

### 3.3 Artificial Photosynthesis Photoelectrochemical System Design

#### 3.3.1 Tandem cell configuration

Tandem cell configuration is a promising approach to address the issues of single or heterojunction PEC devices for unassisted solar water splitting. In the early stage, tandem PEC devices consisting of a semiconductor and a dye-sensitized solar cell (DSSC) were applied for water splitting. For instance, Kim et al.<sup>167</sup> revealed a tandem cell composed of a WO<sub>3</sub>/Pt photoelectrode connected with a DSSC for unassisted water splitting where the maximum STH efficiency of 0.35% was obtained. Subsequently, a Fe<sub>2</sub>O<sub>3</sub> and WO<sub>3</sub> photoanode with a DSSC in tandem configuration was developed, as illustrated in Fig. 3.<sup>168</sup> Without external bias, the achieved STH efficiencies were 3.10% and 1.17% for the WO<sub>3</sub>/DSSC and Fe<sub>2</sub>O<sub>3</sub>/DSSC tandem systems,

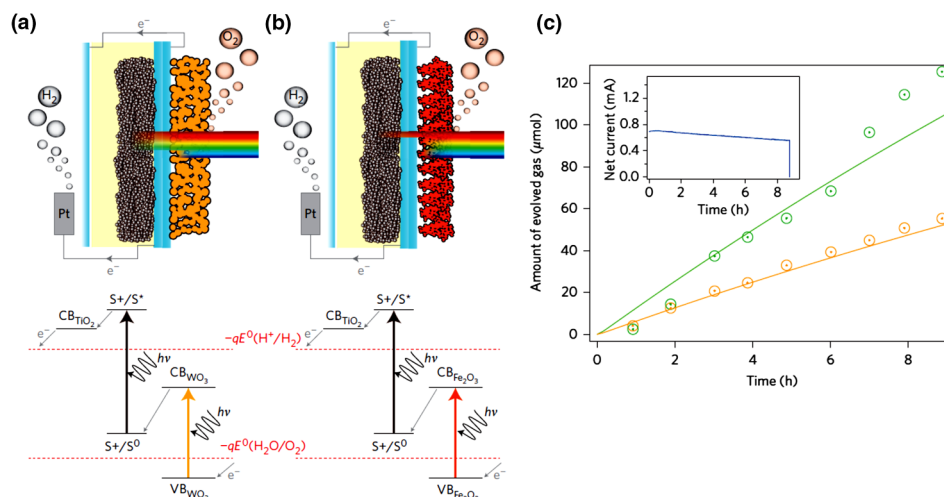


**Fig. 3** Schematic and band energy diagrams represent (a) WO<sub>3</sub>, (b) Fe<sub>2</sub>O<sub>3</sub> photoanodes combined with a DSSC using D4 dye in tandem cell design. Red dotted lines indicate the reduction and oxidation potentials of water and (c) Faradaic efficiency measurement of a tandem cell with inset shows a net measured photocurrent within 9 h. Green and orange circled plots correspond to H<sub>2</sub> and O<sub>2</sub> evolved gases, respectively. Reprinted with permission from Ref. 168. Copyright 2011 Nature Publishing Group.

respectively. The low STH efficiency in this tandem configuration is due to the mismatched band energy configuration and interfacial charge recombination between photoelectrodes and the combined DSSCs. Especially, charge recombination occurred between the injected electrons from the semiconductors and the oxidized dye ( $I_3^-$ ), inhibiting the efficient redox reaction with water in the system.

More recently, an efficient wireless monolithic tandem device consisting of a bipolar configuration with a highly transparent  $\text{BiVO}_4$ -sensitized mesoporous  $\text{WO}_3/\text{Pt}$  film and a porphyrin-dye-based photoelectrode was reported.<sup>169</sup> An extraordinarily high STH efficiency of 5.7% and  $\text{H}_2/\text{O}_2$  evolutions were revealed without any applied bias. The porphyrin-dye-sensitized photoanode with a cobalt electrolyte generated sufficient bias to drive the water splitting reaction forward in this monolithic tandem configuration. Although the efficient design for AP is controversial, the combination of abundant metal oxide-based photoelectrodes with DSSCs has been explored as a promising PEC device configuration for unassisted solar water splitting. Nevertheless, the DSSC component generates low voltages that are not sufficient for water splitting, and more attention has been paid to recently developed PSCs due to their much higher  $V_{oc}$  (0.9 to 1.5 V).<sup>170</sup> For instance, a dual artificial-leaf-type tandem PEC device composed of a robust cobalt carbonate (Co-Ci)-catalyzed Mo-doped  $\text{BiVO}_4$  photoanode and a  $\text{CH}_3\text{NH}_3\text{PbI}_3$ -based PSCs (Fig. 4) can deliver a photocurrent density of  $5 \text{ mA cm}^{-2}$  at 1.23 V versus RHE for the unique and stable photoanode and a STH efficiency of 3.0% for the wireless device.<sup>171</sup> Gratzel et al. reported a novel PSCs-assisted PEC water splitting system composed of organohalide  $\text{CH}_3\text{NH}_3\text{PbI}_3$ -based PSCs as the external power supply and NiFe-layered double hydroxides as the catalytic electrodes, which achieved a photocurrent density of  $\sim 10 \text{ mA cm}^{-2}$  with a STH efficiency of 12.3%.<sup>165</sup> Although this device configuration exhibited a high efficiency for PEC water splitting, the electrodes were not directly settled in photoreactions. Consequently, the hydrogen generation occurred by a water electrolysis process that power was generated through the externally wired two PSCs in series. Meanwhile, a monolithic tandem design with only one  $\text{CH}_3\text{NH}_3\text{PbI}_3$  PSC/Ni layer without an external wire connection was developed and a high photocurrent density of  $12 \text{ mA cm}^{-2}$  was achieved (Fig. 5).<sup>166</sup> Overall, the device complexity and stability issue of the dye and organohalide perovskite materials in the DSSCs and PSCs, and efficient photon utilization should be considered in these design concepts.

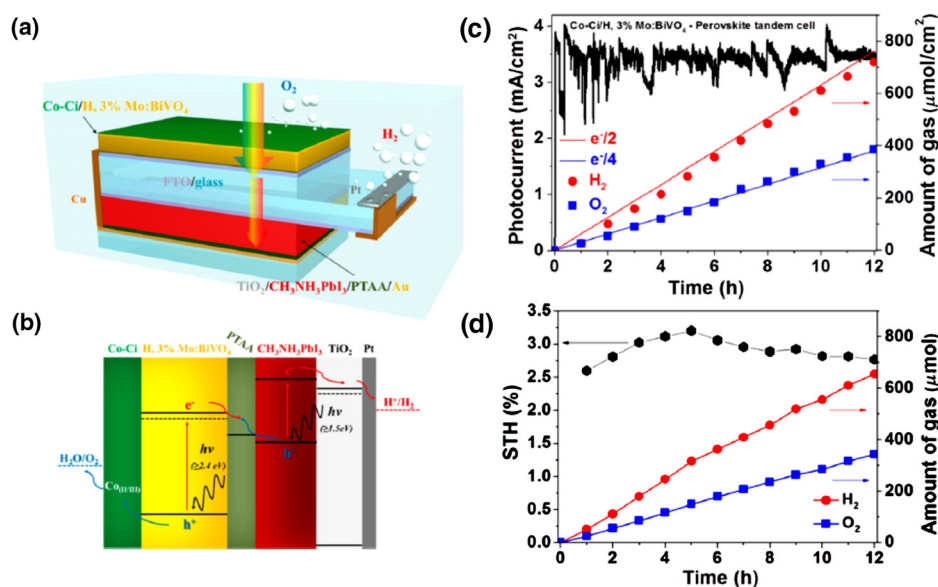


**Fig. 4** Schematic diagrams of (a) wireless dual light absorber tandem PEC device, (b) energy band diagram and charge transfer in artificial water splitting, (c) photocurrent density and  $\text{H}_2/\text{O}_2$  gases evolutions of Co-Ci/H, 3%Mo:BiVO<sub>4</sub> PSC tandem device, and (d) evolved  $\text{H}_2/\text{O}_2$  gases and calculated STH in unassisted solar water splitting. Reprinted with permission from Ref. 171. Copyright 2015 American Chemical Society.



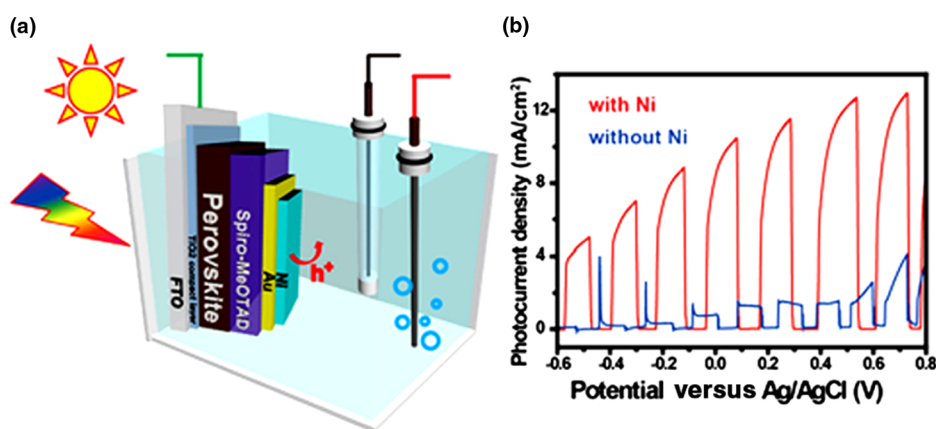


**Fig. 5** (a) Schematic diagrams of  $\text{CH}_3\text{NH}_3\text{PbI}_3$  with Ni surface layer tandem cell configuration and (b) photocurrent densities in unassisted hydrogen production at 1 sun illumination. Reprinted with permission from Ref. 166. Copyright 2015, American Chemical Society.

On the other hand, coupling a PEC device with a PV cell in tandem was developed to extend the light absorption range and improve the photocurrent density in unassisted solar water splitting. Ding et al.<sup>172</sup> achieved a STH efficiency up to 2.5% in an unassisted water splitting system using an earth-abundant photoanode and a Si-solar-cell-based photocathode (Fig. 6). The parallel irradiation mode exhibited higher efficiency than the tandem illumination one because the former system offered sufficient driving force for water splitting. More recently, an overall STH efficiency of 0.91% was achieved on a system composed of a  $\text{Fe}_2\text{O}_3$  photoanode and a Si photocathode with  $\text{NiFeO}_x$  and  $\text{TiO}_2/\text{Pt}$  as cocatalysts (Fig. 7).<sup>173</sup>

### 3.3.2 Monolithic design

Despite continuing efforts on searching various photoanode materials to combine with solar cells, the high current densities are accompanied with the challenges of photocorrosion or chemical instability under oxidative conditions. A stand-alone unassisted PEC device would be an ultimate consideration for  $\text{H}_2/\text{O}_2$  evolutions in water splitting. Accordingly, simpler concepts using dual-absorber tandem devices have been explored with acceptable STH efficiencies. For

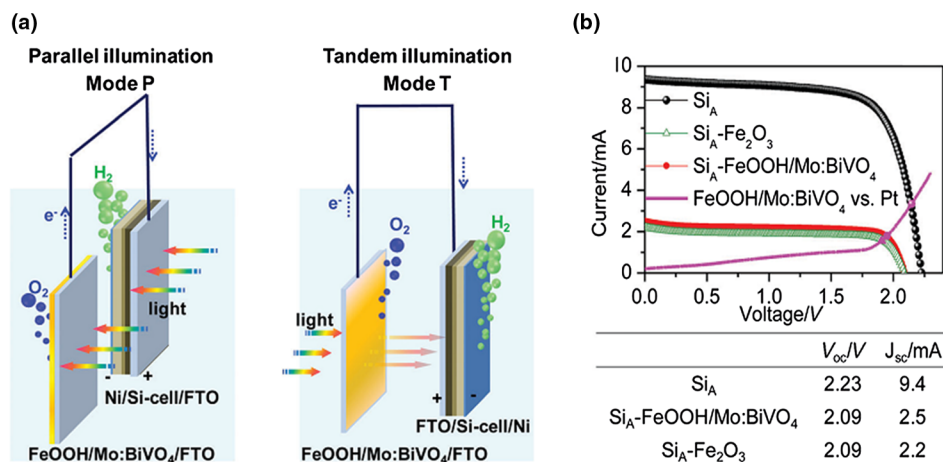


**Fig. 6** (a) Schematic diagram of  $\text{FeOOH/Mo:BiVO}_4$  photoanode with the Ni/Si-solar-cell-based photocathode under parallel and tandem light illumination for direct water splitting and (b)  $I$ - $V$  curves and obtained values of photoelectrodes measured in 0.5M  $\text{Na}_2\text{SO}_4$  electrolyte and two electrode configurations under AM 1.5G light illumination. Reprinted with permission from Ref. 172. Copyright 2014, Royal Society of Chemistry.

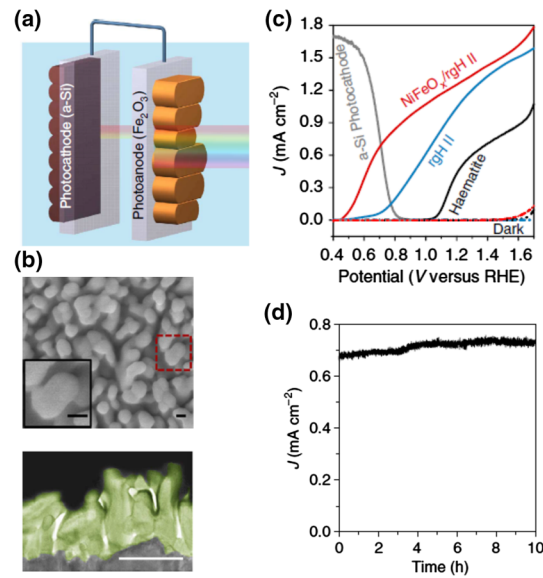


**Fig. 7** (a) Schematic diagrams of Fe<sub>2</sub>O<sub>3</sub> photoanode and amorphous Si photocathode tandem device for overall unassisted water splitting, (b) SEM image of a tandem photoelectrode, (c) current–potential ( $J$ – $V$ ) curves of various photoelectrodes, and (d) net photocurrent of NiFeO<sub>x</sub>-modified second regrowth treatment (rgH II) with TiO<sub>2</sub>/Pt loaded amorphous silicon photocathode over 10 h in 0.5M phosphate solution in a unassisted two-electrode system. Reprinted with permission from Ref. 173. Copyright 2015 Nature Publishing Group.

example, a p-n junction photoelectrode comprising p-type Cu-Ti-O and n-type TiO<sub>2</sub> nanotube arrays with efficient spectral photoresponse (380 to 885 nm) and antiphotocorrosion properties can result in a significantly enhanced photocurrent density of  $\sim 0.25$  mA cm<sup>-2</sup> and a photoconversion efficiency of 0.30% under global AM 1.5 G illumination (Fig. 8).<sup>174</sup> Similarly, a Mn-oxide–TiO<sub>2</sub> coated triple junction-amorphous-Si (Tj-a-Si) was used for monolithic self-driven water splitting with a high STH efficiency of 3.25% and good long-term stability under solar-simulated light illumination.<sup>175</sup>

In a parallel study, Reece et al.<sup>151</sup> reported a Tj-a-Si system modified with cocatalysts for water splitting. The wireless configuration of a Tj-a-Si with Co-oxygen-evolving complex and

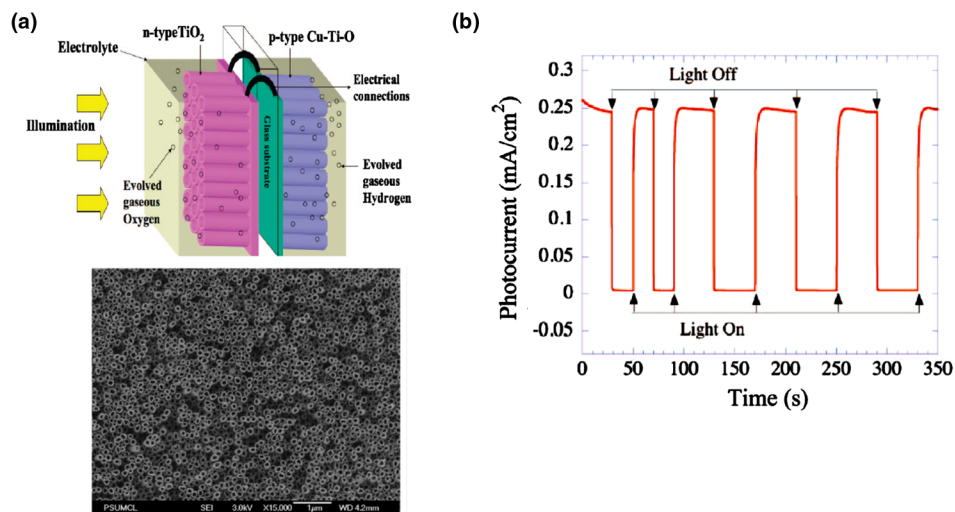


**Fig. 8** (a) Schematic illustration of the n-type TiO<sub>2</sub>/p-type Cu-Ti-O nanotube arrays in tandem with a salt bridge and immersed in hybrid electrolyte containing 1 M KOH and 0.1 M Na<sub>2</sub>HPO<sub>4</sub> and (b) Self-biased photocurrent density of the n-type TiO<sub>2</sub>/p-type Cu-Ti-O nanotube arrays in tandem under global AM 1.5 G illumination. Reprinted with permission from Ref. 174. Copyright 2008 American Chemical Society.

NiMoZn as OER and HER cocatalysts presented a high STH efficiency of 4.7% under AM 1.5 G simulated sunlight illumination. It has been confirmed that this design can generate electrons and holes with enough energy to split water ( $V_{OC} > 1.23$  V) in a simply engineered configuration. However, the high cost of the photoelectrode materials and the complexity of the fabrication process would be critical limiting factors in commercializing this water splitting system.

### 3.3.3 Heterojunction components of photoelectrochemical device design

Most studies have been focused on improving the performance of individual semiconductors to achieve the targeted STH efficiency. However, the performance of the whole PEC system and the interaction between the individual components for solar energy conversion should also be explored. Liu et al.<sup>79</sup> reported a fully integrated nanotree PEC system consisting of cocatalysts loaded Si and TiO<sub>2</sub> nanowires for direct solar water splitting (Fig. 9). An STH efficiency of 0.12% was achieved in this unassisted PEC water splitting system. However, this nanotree PEC system still needs to improve the current density and maximize the STH efficiency via excellent interfacial engineering and surface modifications. More recently, a tandem PEC system consisting of a n-p homojunction of Si microwire arrays coated with TiO<sub>2</sub> thin films presented a current density of 0.32 mA cm<sup>-2</sup> and a STH efficiency of 0.6% without external bias (Fig. 10).<sup>176</sup> It is well known that the use of Si photoelectrodes in a PEC water splitting system reduces the cost competitiveness, thus novel systems with low cost materials have continuously been explored.

Another promising concept for unassisted PEC water splitting systems is a standalone Z-scheme configuration. To obtain high performance, we need to consider the main factors, in particular, the design of the fully integrated system, the functions of the individual materials, and the optimization of the interfaces between the individual components.<sup>177</sup> One typical example is the design of W/Mo-doped BiVO<sub>4</sub> and Zn<sub>x</sub>Cd<sub>1-x</sub>Se dual n-type photoelectrode system with the presence of redox mediators ( $I^-/IO_3^-$  or  $S^{2-}/S_n^{2-}$ ),<sup>178</sup> which highlights the challenging nature of designing redox mediator-free Z-scheme systems via metal doping and surface modification for efficient water splitting. Likewise, Yang et al.<sup>179</sup> studied the surface modification with different catalysts in order to improve the overall water splitting efficiency and stability of the system (Fig. 11). They designed a system comprising a CdS QD/TiO<sub>2</sub> nanorod photoanode and a ZnS/CdSe QD/NiO<sub>x</sub> nanosheet photocathode for self-driven PEC water splitting,

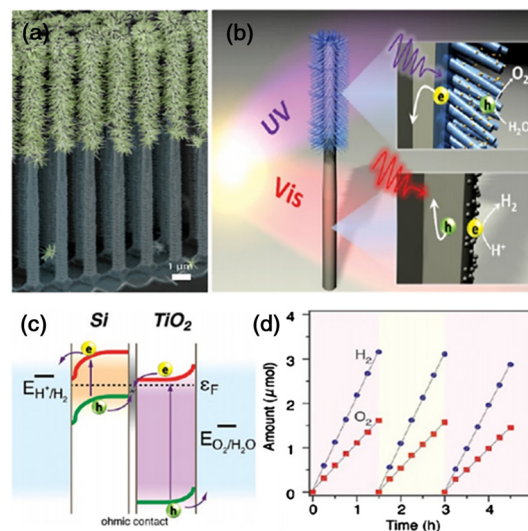


**Fig. 9** (a) SEM image of the Si/TiO<sub>2</sub> heterostructure nanotree arrays photoelectrodes, (b, c) Schematic illustrations of the light absorption and charge transfer of Si/TiO<sub>2</sub> photoelectrodes in unassisted water splitting reaction, and (d) the evolution of H<sub>2</sub> and O<sub>2</sub> with 2:1 stoichiometry under simulated sunlight (1.5 suns) Reprinted with permission from Ref. 79. Copyright 2013 American Chemical Society.

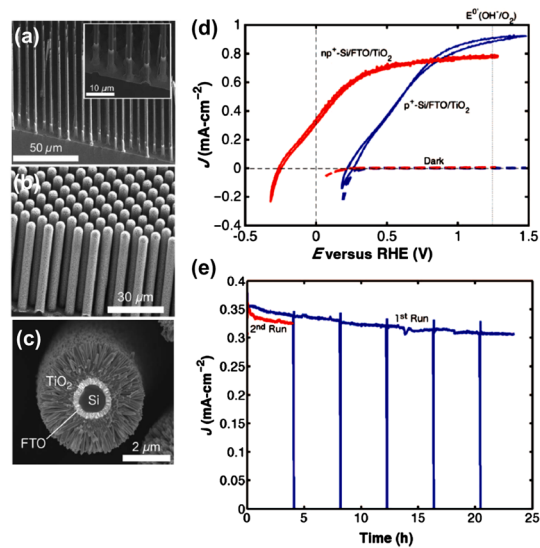


**Fig. 10** SEM images of (a) n-p homojunction of Si microwire array (inset shows a zoomed-in image of the SiO<sub>2</sub> microwires), (b) FTO-coated n-p homojunction of Si microwire array, and (c) cross-section of TiO<sub>2</sub>-coated n-p Si/FTO microwire array. (d) Current density versus potential curves of p<sup>+</sup>-Si/FTO/TiO<sub>2</sub> and n-p Si/FTO/TiO<sub>2</sub> microwire array photoelectrodes and (e) amperometric curves of n-p Si/FTO/TiO<sub>2</sub> microwire array photoelectrodes at 0 V versus RHE under the dark and 1 sun light illumination conditions. Reprinted with permission from Ref. 176. Copyright 2016, The Electrochemical Society.

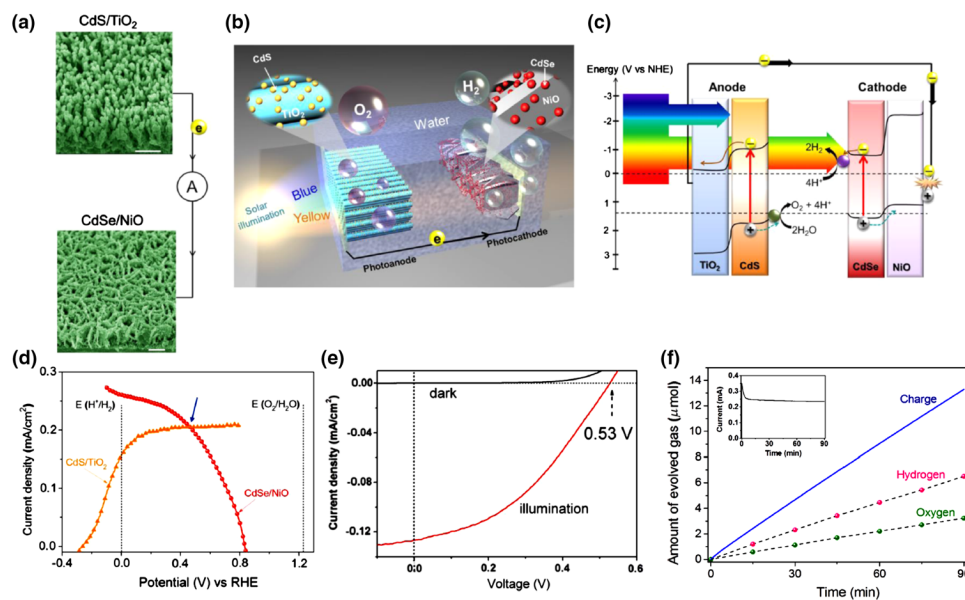


**Fig. 11** (a) SEM images of CdS QD/TiO<sub>2</sub> nanorod photoanode (top) and CdSe QD/NiO nanosheet photocathode (bottom) (scale bar: 500 nm), (b) schematic representation of PEC device configuration, (c) band diagram and charge transfer in heterojunction photoelectrodes, (d) amperometric curves of CdS QD/TiO<sub>2</sub> nanorod photoanode and CdSe QD/NiO nanosheet in 0.5 M Na<sub>2</sub>SO<sub>4</sub> electrolyte, (e) J–V curve of CdS QD/TiO<sub>2</sub> nanorod photoanode and CdSe QD/NiO nanosheet photocathode in unbiased water splitting, and (f) hydrogen and oxygen gases evolutions and inset presents stability of the photocurrent under 90-min light illuminations. Reprinted with permission from Ref. 179. Copyright 2014 American Chemical Society.

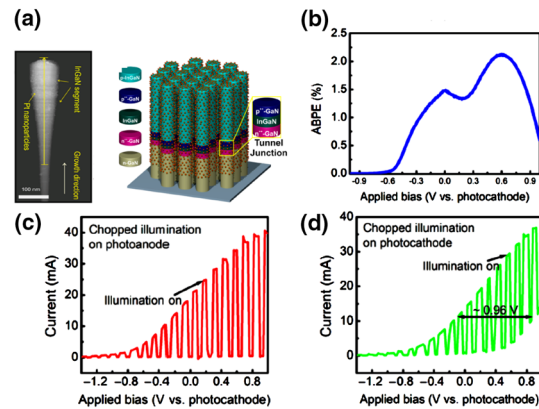


**Fig. 12** (a) STEM-HAADF image of a single Pt-InGaN nanowire and schematic of the p-InGaN nanowire photocathode and n-Si substrate, in which connected directly in tunnel junction, (b) the solar conversion efficiency of the dual-photoelectrodes as a function of applied bias under AM1.5G 1 sun illumination,  $I-V$  curve of the dual-photoelectrode device with the (c) photoanode and (d) photocathode under chopped illumination. Reprinted with permission from Ref. 180. Copyright 2015 American Chemical Society.

which delivered a maximum STH efficiency of 0.17%, comparable to natural photosynthesis. Later, a system composed of dual nanowire photoelectrodes of p-InGaN/Si-InGaN was developed, where a STH efficiency of 2% at 0.6 V versus RHE and a high open circuit potential were achieved under AM 1.5 G 1 sun illumination (Fig. 12).<sup>180</sup> Nevertheless, this design requires expensive and rare cocatalysts to drive the solar water splitting reaction. Therefore, other active and cheaper semiconductors and cocatalysts for overall water splitting should be explored in future studies.

## 4 Summary and Perspectives

In this review article, we provided an overview of a library of PEC system designs toward unassisted solar water splitting. It is clear that the design of efficient unassisted PEC devices relies not only on material design but also the integration of PEC configuration. In particular, the development of semiconductors via novel nanostructure engineering, surface modification with exotic element doping or cocatalyst loading, and innovative system design based on heterojunction configurations are important strategies for improving light harvesting, charge separation, and surface reaction kinetics. This brief review would deliver useful information for further construction and development of efficient unassisted PEC water splitting systems with high STH efficiency, long-term stability, and low cost. For example, the stability and poor kinetics of water splitting issues in the wireless integrated tandem system with dual light absorber configuration should be addressed by employing earth abundant materials, protective layers, and morphology engineering techniques. On the other hand, novel strategies to inhibit photocorrosion of the photocathode materials are urgently needed for efficient water splitting in a long-term period. Additionally, the tandem system combining semiconductors with a PV device has a conflict in terms of instability in aqueous electrolyte, high cost and complexity. Using DSSCs or PSCs in tandem systems for unassisted water splitting demonstrates low cost and comparable STH efficiencies, but the efficient light absorption and stable organic dyes for DSSCs and the stability of perovskites should be considered when equipped in a PEC system.

Although numerous achievements have been obtained in recent years, it is still highly challenging to develop an efficient unassisted PEC water splitting system for practical applications. Currently, the tentative STH goal for practical applications of the unassisted PEC water splitting device is 10%. It is expected that some novel concepts of fully integrated PEC devices put forward the breakthrough in solar hydrogen energy conversion and long-term stability. Notably, the Z-scheme concept for unassisted PEC water splitting systems is promising for effective photon utilization and efficient solar water splitting. However, there still remains significant room for the improvement of this system for practical applications. It is also important to explore new active



and low cost cocatalysts that can efficiently promote the forward reactions for water splitting. To this end, in-depth understanding of the mechanisms of unassisted PEC water splitting and the strategies to boost charge transfer and separation for redox reaction is critically important to develop an efficient solar water splitting system for more sustainable solar energy utilization.

## Acknowledgments

The authors would like to acknowledge financial support from the Australian Research Council through its DP and FF programs. P.P. acknowledges support from the University of Queensland for International Scholarships (UQI). S.W. acknowledges support from IPRS and UQ Centennial Scholarships.

## References

1. R. Abe, "Recent progress on photocatalytic and photoelectrochemical water splitting under visible light irradiation," *J. Photochem. Photobiol. C* **11**, 179–209 (2010).
2. M. Gratzel, "Photoelectrochemical cells," *Nature* **414**, 338–344 (2001).
3. A. Fujishima and K. Honda, "Electrochemical photolysis of water at a semiconductor electrode," *Nature* **238**, 37–38 (1972).
4. C. Zhen et al., "Tantalum (oxy)nitride based photoanodes for solar-driven water oxidation," *J. Mater. Chem. A* **4**, 2783–2800 (2016).
5. X. Zong and L. Z. Wang, "Ion-exchangeable semiconductor materials for visible light-induced photocatalysis," *J. Photochem. Photobiol. C* **18**, 32–49 (2014).
6. Q. Wang et al., "Scalable water splitting on particulate photocatalyst sheets with a solar-to-hydrogen energy conversion efficiency exceeding 1%," *Nat. Mater.* **15**, 611–615 (2016).
7. T. Hisatomi et al., "Enhancement in the performance of ultrathin hematite photoanode for water splitting by an oxide underlayer," *Adv. Mater.* **24**, 2699–2702 (2012).
8. Y. Li and J. Z. Zhang, "Hydrogen generation from photoelectrochemical water splitting based on nanomaterials," *Laser Photonics Rev.* **4**, 517–528 (2010).
9. A. Kudo and Y. Miseki, "Heterogeneous photocatalyst materials for water splitting," *Chem. Soc. Rev.* **38**, 253–278 (2009).
10. M. G. Walter et al., "Solar water splitting cells," *Chem. Rev.* **110**, 6446–6473 (2010).
11. G. Liu et al., "Enhanced photoactivity of oxygen-deficient anatase TiO<sub>2</sub> sheets with dominant {001} facets," *J. Phys. Chem. C* **113**, 21784–21788 (2009).
12. G. Liu et al., "Titania-based photocatalysts—crystal growth, doping and heterostructuring," *J. Mater. Chem.* **20**, 831–843 (2010).
13. L. Xing et al., "Pt modified TiO<sub>2</sub> nanotubes electrode: preparation and electrocatalytic application for methanol oxidation," *Int. J. Hydrogen Energy* **35**, 12169–12173 (2010).
14. J. Gu et al., "Water reduction by a p-GaInP<sub>2</sub> photoelectrode stabilized by an amorphous TiO<sub>2</sub> coating and a molecular cobalt catalyst," *Nat. Mater.* **15**, 456–460 (2016).
15. S. Y. Noh et al., "Branched TiO<sub>2</sub>/Si nanostructures for enhanced photoelectrochemical water splitting," *Nano Energy* **2**, 351–360 (2013).
16. N. Srinivasan, E. Sakai, and M. Miyauchi, "Balanced excitation between two semiconductors in bulk heterojunction Z-scheme system for overall water splitting," *ACS Catal.* **6**, 2197–2200 (2016).
17. Y. H. Lai, D. W. Palm, and E. Reisner, "Multifunctional coatings from scalable single source precursor chemistry in tandem photoelectrochemical water splitting," *Adv. Energy Mater.* **5**, 1501668 (2015).
18. F. Jiang et al., "Pt/In<sub>2</sub>S<sub>3</sub>/CdS/Cu<sub>2</sub>ZnSnS<sub>4</sub> thin film as an efficient and stable photocathode for water reduction under sunlight radiation," *J. Am. Chem. Soc.* **137**, 13691–13697 (2015).
19. F. F. Abdi et al., "Efficient solar water splitting by enhanced charge separation in a bismuth vanadate-silicon tandem photoelectrode," *Nat. Commun.* **4**, 2195 (2013).
20. J. Brilliet et al., "Highly efficient water splitting by a dual-absorber tandem cell," *Nat. Photonics* **6**, 824–828 (2012).



21. H. S. Jeon et al., "A monolithic and standalone solar-fuel device having comparable efficiency to photosynthesis in nature," *J. Mater. Chem. A* **3**, 5835–5842 (2015).
22. J. H. Park and A. J. Bard, "Photoelectrochemical tandem cell with bipolar dye-sensitized electrodes for vectorial electron transfer for water splitting," *Electrochem. Solid-State Lett.* **9**, E5–E8 (2006).
23. E. L. Miller, R. E. Rocheleau, and S. Khan, "A hybrid multijunction photoelectrode for hydrogen production fabricated with amorphous silicon/germanium and iron oxide thin films," *Int. J. Hydrogen Energy* **29**, 907–914 (2004).
24. O. Khaselev and J. A. Turner, "A monolithic photovoltaic-photoelectrochemical device for hydrogen production via water splitting," *Science* **280**, 425–427 (1998).
25. R. E. Rocheleau, E. L. Miller, and A. Misra, "High-efficiency photoelectrochemical hydrogen production using multijunction amorphous silicon photoelectrodes," *Energy Fuels* **12**, 3–10 (1998).
26. E. Verlage et al., "A monolithically integrated, intrinsically safe, 10% efficient, solar-driven water-splitting system based on active, stable earth-abundant electrocatalysts in conjunction with tandem III-V light absorbers protected by amorphous TiO<sub>2</sub> films," *Energy Environ. Sci.* **8**, 3166–3172 (2015).
27. J. W. Ager et al., "Experimental demonstrations of spontaneous, solar-driven photoelectrochemical water splitting," *Energy Environ. Sci.* **8**, 2811–2824 (2015).
28. D. Kim et al., "Artificial photosynthesis for sustainable fuel and chemical production," *Angew. Chem. Int. Ed.* **54**, 3259–3266 (2015).
29. Y. Tachibana, L. Vayssieres, and J. R. Durrant, "Artificial photosynthesis for solar water-splitting," *Nat. Photonics* **6**, 511–518 (2012).
30. T. Faunce et al., "Artificial photosynthesis as a frontier technology for energy sustainability," *Energy Environ. Sci.* **6**, 1074 (2013).
31. A. J. Bard and M. A. Fox, "Artificial photosynthesis: solar splitting of water to hydrogen and oxygen," *Acc. Chem. Res.* **28**, 141–145 (1995).
32. S. S. Mao and S. Shen, "Hydrogen production: catalysing artificial photosynthesis," *Nat. Photonics* **7**, 944–946 (2013).
33. I. McConnell, G. Li, and G. W. Brudvig, "Energy conversion in natural and artificial photosynthesis," *Chem. Biol.* **17**, 434–447 (2010).
34. S. Shen and S. S. Mao, "Nanostructure designs for effective solar-to-hydrogen conversion," *Nanophotonics* **1**, 31–50 (2012).
35. H. Chen and L. Wang, "Nanostructure sensitization of transition metal oxides for visible-light photocatalysis," *Beilstein J. Nanotechnol.* **5**, 696–710 (2014).
36. S. Wang et al., "Synergistic crystal facet engineering and structural control of WO<sub>3</sub> films exhibiting unprecedented photoelectrochemical performance," *Nano Energy* **24**, 94–102 (2016).
37. P. Peerakiatkhajohn et al., "Stable hematite nanosheet photoanodes for enhanced photoelectrochemical water splitting," *Adv. Mater.* **28**, 6405–6410 (2016).
38. Y. Kuang et al., "A front-illuminated nanostructured transparent BiVO<sub>4</sub> photoanode for >2% efficient water splitting," *Adv. Energy Mater.* **6**, 1501645 (2016).
39. B. J. Trzeźniewski and W. A. Smith, "Photocharged BiVO<sub>4</sub> photoanodes for improved solar water splitting," *J. Mater. Chem. A* **4**, 2919–2926 (2016).
40. X. Zong et al., "A scalable colloidal approach to prepare hematite films for efficient solar water splitting," *Phys. Chem. Chem. Phys.* **15**, 12314–12321 (2013).
41. P. Zhou, J. Yu, and M. Jaroniec, "All-solid-state Z-scheme photocatalytic systems," *Adv. Mater.* **26**, 4920–4935 (2014).
42. W. Wang et al., "Si:WO<sub>3</sub> heterostructure for Z-scheme water splitting: an AB initio study," *J. Mater. Chem. A* **1**, 1078–1085 (2013).
43. P. Peerakiatkhajohn et al., "A hybrid photoelectrode with plasmonic Au at TiO<sub>2</sub> nanoparticles for enhanced photoelectrochemical water splitting," *J. Mater. Chem. A* **3**, 20127–20133 (2015).
44. T. Kothe et al., "Combination of a photosystem 1-based photocathode and a photosystem 2-based photoanode to a Z-scheme mimic for biophotovoltaic applications," *Angew. Chem. Int. Ed.* **52**, 14233–14236 (2013).

45. R. M. Navarro, F. del Valle, and J. L. G. Fierro, "Photocatalytic hydrogen evolution from CdS-ZnO-CdO systems under visible light irradiation: effect of thermal treatment and presence of Pt and Ru cocatalysts," *Inter. J. Hydrogen Energy* **33**, 4265–4273 (2008).
46. K. Maeda, "Z-scheme water splitting using two different semiconductor photocatalysts," *ACS Catal.* **3**, 1486–1503 (2013).
47. Q. Wang et al., "Core/shell structured La- and Rh-codoped SrTiO<sub>3</sub> as a hydrogen evolution photocatalyst in Z-scheme overall water splitting under visible light irradiation," *Chem. Mater.* **26**, 4144–4150 (2014).
48. S. Chen et al., "Efficient visible-light-driven Z-scheme overall water splitting using a MgTa<sub>2</sub>O(6-x)N(y)/TaON heterostructure photocatalyst for H<sub>2</sub> evolution," *Angew. Chem. Int. Ed.* **54**, 8498–8501 (2015).
49. Y. Sasaki, H. Kato, and A. Kudo, "[Co(bpy)<sub>3</sub>]<sup>(3+/2+)</sup> and [Co(phen)<sub>3</sub>]<sup>(3+/2+)</sup> electron mediators for overall water splitting under sunlight irradiation using Z-scheme photocatalyst system," *J. Am. Chem. Soc.* **135**, 5441–5449 (2013).
50. X. Wang et al., "ZnO-CdS at Cd heterostructure for effective photocatalytic hydrogen generation," *Adv. Energy Mater.* **2**, 42–46 (2012).
51. X. Wang et al., "Enhanced photocatalytic hydrogen evolution by prolonging the lifetime of carriers in ZnO/CdS heterostructures," *Chem. Commun.* (23), 3452–3454 (2009).
52. K. S. Joya et al., "Water-splitting catalysis and solar fuel devices: artificial leaves on the move," *Angew. Chem. Int. Ed.* **52**, 10426–10437 (2013).
53. D. G. Nocera, "The artificial leaf," *Acc. Chem. Res.* **45**, 767–776 (2012).
54. H. Zhou et al., "Artificial inorganic leaves for efficient photochemical hydrogen production inspired by natural photosynthesis," *Adv. Mater.* **22**, 951–956 (2010).
55. Y. Tachibana, L. Vayssieres, and J. R. Durrant, "Artificial photosynthesis for solar water-splitting," *Nat. Photonics* **6**, 511–518 (2012).
56. F. E. Osterloh, "Inorganic nanostructures for photoelectrochemical and photocatalytic water splitting," *Chem. Soc. Rev.* **42**, 2294–2320 (2013).
57. V. Antonucci, E. Passalacqua, and N. Giordano, "TiO<sub>2</sub>-based photoelectrodes in photoelectrochemical cells: performance and mechanism of O<sub>2</sub> evolution," *Int. J. Hydrogen Energy* **12**, 305–313 (1987).
58. T.-T. Duong et al., "Enhanced photoelectrochemical activity of the TiO<sub>2</sub>/ITO nanocomposites grown onto single-walled carbon nanotubes at a low temperature by nanocluster deposition," *Adv. Mater.* **23**, 5557–5562 (2011).
59. S. Higashimoto, M. Sakiyama, and M. Azuma, "Photoelectrochemical properties of hybrid WO<sub>3</sub>/TiO<sub>2</sub> electrode. Effect of structures of WO<sub>3</sub> on charge separation behavior," *Thin Solid Films* **503**, 201–206 (2006).
60. B. D. Alexander et al., "Metal oxide photoanodes for solar hydrogen production," *J. Mater. Chem.* **18**, 2298–2303 (2008).
61. J. Brillet et al., "Examining architectures of photoanode-photovoltaic tandem cells for solar water splitting," *J. Mater. Res.* **25**, 17–24 (2010).
62. R. P. Antony et al., "Efficient photocatalytic hydrogen generation by Pt modified TiO<sub>2</sub> nanotubes fabricated by rapid breakdown anodization," *Int. J. Hydrogen Energy* **37**, 8268–8276 (2012).
63. B.-R. Kim et al., "Effect of TiO<sub>2</sub> supporting layer on Fe<sub>2</sub>O<sub>3</sub> photoanode for efficient water splitting," *Progr. Org. Coat.* **76**, 1869–1873 (2013).
64. C. W. Lai and S. Sreekantan, "Preparation of hybrid WO<sub>3</sub>-TiO<sub>2</sub> nanotube photoelectrodes using anodization and wet impregnation: improved water-splitting hydrogen generation performance," *Int. J. Hydrogen Energy* **38**, 2156–2166 (2013).
65. V. K. Mahajan, S. K. Mohapatra, and M. Misra, "Stability of TiO<sub>2</sub> nanotube arrays in photoelectrochemical studies," *Int. J. Hydrogen Energy* **33**, 5369–5374 (2008).
66. J. A. Seabold et al., "Photoelectrochemical properties of heterojunction CdTe/TiO<sub>2</sub> electrodes constructed using highly ordered TiO<sub>2</sub> nanotube arrays," *Chem. Mater.* **20**, 5266–5273 (2008).
67. J. Su et al., "Nanostructured WO<sub>3</sub>/BiVO<sub>4</sub> heterojunction films for efficient photoelectrochemical water splitting," *Nano. Lett.* **11**, 1928–1933 (2011).

68. S. J. Moniz et al., "1D Co-Pi modified BiVO<sub>4</sub>/ZnO junction cascade for efficient photoelectrochemical water cleavage," *Adv. Energy Mater.* **4**, 1301590 (2014).
69. L. Liang et al., "High-performance flexible electrochromic device based on facile semiconductor-to-metal transition realized by WO<sub>3</sub> · 2H<sub>2</sub>O ultrathin nanosheets," *Sci. Rep.* **3**, 1936 (2013).
70. J. Liu et al., "Highly oriented Ge-doped hematite nanosheet arrays for photoelectrochemical water oxidation," *Nano Energy* **9**, 282–290 (2014).
71. M. Ji et al., "Controlled growth of ferrihydrite branched nanosheet arrays and their transformation to hematite nanosheet arrays for photoelectrochemical water splitting," *ACS Appl. Mater. Interfaces* **8**, 3651–3660 (2016).
72. I. Y. Kim et al., "Unique advantages of exfoliated 2D nanosheets for tailoring the functionalities of nanocomposites," *J. Phys. Chem. Lett.* **5**, 4149–4161 (2014).
73. B. Seger et al., "An n-type to p-type switchable photoelectrode assembled from alternating exfoliated titania nanosheets and polyaniline layers," *Angew. Chem. Int. Ed.* **52**, 6400–6403 (2013).
74. K. Sun et al., "3D branched nanowire heterojunction photoelectrodes for high-efficiency solar water splitting and H<sub>2</sub> generation," *Nanoscale* **4**, 1515–1521 (2012).
75. J. Shen et al., "3D hierarchical ZnIn<sub>2</sub>S<sub>4</sub>: the preparation and photocatalytic properties on water splitting," *Int. J. Hydrogen Energy* **37**, 16986–16993 (2012).
76. Z. Zheng et al., "CdS sensitized 3D hierarchical TiO<sub>2</sub>/ZnO heterostructure for efficient solar energy conversion," *Sci. Rep.* **4**, 5721 (2014).
77. V. Chakrapani, J. Thangala, and M. K. Sunkara, "WO<sub>3</sub> and W<sub>2</sub>N nanowire arrays for photoelectrochemical hydrogen production," *Int. J. Hydrogen Energy* **34**, 9050–9059 (2009).
78. M. Frites, Y. A. Shaban, and S. U. Khan, "Iron oxide (n-Fe<sub>2</sub>O<sub>3</sub>) nanowire films and carbon modified (CM)-n-Fe<sub>2</sub>O<sub>3</sub> thin films for hydrogen production by photosplitting of water," *Int. J. Hydrogen Energy* **35**, 4944–4948 (2010).
79. C. Liu et al., "A fully integrated nanosystem of semiconductor nanowires for direct solar water splitting," *Nano Lett.* **13**, 2989–2992 (2013).
80. H.-J. Ahn et al., "Nanoporous hematite structures to overcome short diffusion lengths in water splitting," *J. Mater. Chem. A* **2**, 19999–20003 (2014).
81. X. Guo, L. Wang, and Y. Tan, "Hematite nanorods Co-doped with Ru cations with different valence states as high performance photoanodes for water splitting," *Nano Energy* **16**, 320–328 (2015).
82. Z. Su et al., "Hydrothermal growth of highly oriented single crystalline Ta<sub>2</sub>O<sub>5</sub> nanorod arrays and their conversion to Ta<sub>3</sub>N<sub>5</sub> for efficient solar driven water splitting," *Chem. Commun.* **50**, 15561–15564 (2014).
83. H. Dang et al., "TiO<sub>2</sub> nanotubes coupled with nano-Cu(OH)<sub>2</sub> for highly efficient photocatalytic hydrogen production," *Int. J. Hydrogen Energy* **38**, 2126–2135 (2013).
84. A. Ghicov et al., "TiO<sub>2</sub>-Nb<sub>2</sub>O<sub>5</sub> nanotubes with electrochemically tunable morphologies," *Angew. Chem. Int. Ed.* **45**, 6993–6996 (2006).
85. Y. Liu et al., "Highly stable CdS-modified short TiO<sub>2</sub> nanotube array electrode for efficient visible-light hydrogen generation," *Int. J. Hydrogen Energy* **36**, 167–174 (2011).
86. Y. Lai, J. Gong, and C. Lin, "Self-organized TiO<sub>2</sub> nanotube arrays with uniform platinum nanoparticles for highly efficient water splitting," *Int. J. Hydrogen Energy* **37**, 6438–6446 (2012).
87. L. Wang and T. Sasaki, "Titanium oxide nanosheets: graphene analogues with versatile functionalities," *Chem. Rev.* **114**, 9455–9486 (2014).
88. B. Luo, G. Liu, and L. Wang, "Recent advances in 2D materials for photocatalysis," *Nanoscale* **8**, 6904–6920 (2016).
89. M. Zhou, X. W. Lou, and Y. Xie, "Two-dimensional nanosheets for photoelectrochemical water splitting: possibilities and opportunities," *Nano Today* **8**(6), 598–618 (2013).
90. S. Yamada, A. Y. Nosaka, and Y. Nosaka, "Fabrication of CdS photoelectrodes coated with titania nanosheets for water splitting with visible light," *J. Electroanal. Chem.* **585**, 105–112 (2005).
91. J. Zhu et al., "Hierarchical hollow spheres composed of ultrathin Fe<sub>2</sub>O<sub>3</sub> nanosheets for lithium storage and photocatalytic water oxidation," *Energy Environ. Sci.* **6**, 987–993 (2013).

92. Y. Sun et al., "All-surface-atomic-metal chalcogenide sheets for high-efficiency visible-light photoelectrochemical water splitting," *Adv. Energy Mater.* **4**, 1300611 (2014).
93. Y. Sun et al., "Freestanding tin disulfide single-layers realizing efficient visible-light water splitting," *Angew. Chem. Int. Ed.* **51**, 8727–8731 (2012).
94. Y. Sun et al., "Fabrication of flexible and freestanding zinc chalcogenide single layers," *Nat. Commun.* **3**, 1057 (2012).
95. Y. Hou et al., "Branched WO<sub>3</sub> nanosheet array with layered C<sub>3</sub>N<sub>4</sub> heterojunctions and CoO<sub>x</sub> nanoparticles as a flexible photoanode for efficient photoelectrochemical water oxidation," *Adv. Mater.* **26**, 5043–5049 (2014).
96. F. Su et al., "Dendritic Au/TiO<sub>2</sub> nanorod arrays for visible-light driven photoelectrochemical water splitting," *Nanoscale* **5**, 9001–9009 (2013).
97. X. Zhang et al., "Coupling surface plasmon resonance of gold nanoparticles with slow-photon-effect of TiO<sub>2</sub> photonic crystals for synergistically enhanced photoelectrochemical water splitting," *Energy Environ. Sci.* **7**, 1409–1419 (2014).
98. A. G. Tamirat et al., "Efficient photoelectrochemical water splitting using three dimensional urchin-like hematite nanostructure modified with reduced graphene oxide," *J. Power Sources* **287**, 119–128 (2015).
99. Z. Li et al., "A three-dimensional interconnected hierarchical FeOOH/TiO<sub>2</sub>/ZnO nanostructural photoanode for enhancing the performance of photoelectrochemical water oxidation," *Nanoscale* **7**, 19178–19183 (2015).
100. S. W. Boettcher et al., "Photoelectrochemical hydrogen evolution using Si microwire arrays," *J. Am. Chem. Soc.* **133**, 1216–1219 (2011).
101. J. Luo et al., "Cu<sub>2</sub>O nanowire photocathodes for efficient and durable solar water splitting," *Nano Lett.* **16**, 1848–1857 (2016).
102. J. Luo et al., "Solution transformation of CuO into CuInS<sub>2</sub> for solar water splitting," *Nano Lett.* **15**, 1395–1402 (2015).
103. Y.-L. Lee, C.-F. Chi, and S.-Y. Liau, "CdS/CdSe Co-sensitized TiO<sub>2</sub> photoelectrode for efficient hydrogen generation in a photoelectrochemical cell," *Chem. Mater.* **22**, 922–927 (2009).
104. Z. M. Xia et al., "Protection strategy for improved catalytic stability of silicon photoanodes for water oxidation," *Sci. Bull.* **60**, 1395–1402 (2015).
105. W. Siripala et al., "A Cu<sub>2</sub>O/TiO<sub>2</sub> heterojunction thin film cathode for photoelectrocatalysis," *Solar Energy Mater. Solar Cells.* **77**, 229–237 (2003).
106. A. Paracchino et al., "Ultrathin films on copper(i) oxide water splitting photocathodes: a study on performance and stability," *Energy Environ. Sci.* **5**, 8673–8681 (2012).
107. L. Yang et al., "High efficient photocatalytic degradation of p-nitrophenol on a unique Cu<sub>2</sub>O/TiO<sub>2</sub> p-n heterojunction network catalyst," *Environ. Sci. Technol.* **44**, 7641–7646 (2010).
108. R. Marschall and L. Wang, "Non-metal doping of transition metal oxides for visible-light photocatalysis," *Catal. Today* **225**, 111–135 (2014).
109. J.-W. Shi et al., "Carbon-doped titania hollow spheres with tunable hierarchical macroporous channels and enhanced visible light-induced photocatalytic activity," *Chem. Catal. Chem.* **4**, 488–491 (2012).
110. J.-W. Shi et al., "Facile one-pot synthesis of Eu, N-codoped mesoporous titania microspheres with yolk-shell structure and high visible-light induced photocatalytic performance," *Appl. Catal. A* **435–436**, 86–92 (2012).
111. X. Zong et al., "Photocatalytic water oxidation on F, N co-doped TiO<sub>2</sub> with dominant exposed {001} facets under visible light," *Chem. Commun.* **47**, 11742–11744 (2011).
112. X. Zong et al., "Nitrogen doping in ion-exchangeable layered tantalate towards visible-light induced water oxidation," *Chem. Commun.* **47**, 6293–6295 (2011).
113. A. Mukherji et al., "Photocatalytic hydrogen production from water using N-doped Ba<sub>5</sub>Ta<sub>4</sub>O<sub>15</sub> under solar irradiation," *J. Phys. Chem. C* **115**, 15674–15678 (2011).
114. A. Mukherji et al., "Nitrogen doped Sr<sub>2</sub>Ta<sub>2</sub>O<sub>7</sub> coupled with graphene sheets as photocatalysts for increased photocatalytic hydrogen production," *ACS Nano* **5**, 3483–3492 (2011).
115. A. Mukherji et al., "N-Doped CsTaWO<sub>6</sub> as a new photocatalyst for hydrogen production from water splitting under solar irradiation," *Adv. Funct. Mater.* **21**, 126–132 (2011).

116. R. Marschall et al., "Preparation of new sulfur-doped and sulfur/nitrogen co-doped CsTaWO<sub>6</sub> photocatalysts for hydrogen production from water under visible light," *J. Mater. Chem.* **21**, 8871–8879 (2011).
117. J. Wang et al., "Recent progress in cobalt-based heterogeneous catalysts for electrochemical water splitting," *Adv. Mater.* **28**, 215–230 (2016).
118. L. Chen et al., "Enhanced visible photocatalytic activity of hybrid Pt/ $\alpha$ -Fe<sub>2</sub>O<sub>3</sub> nanorods," *RSC Adv.* **2**, 10057–10063 (2012).
119. Z. Li et al., "Triphenylamine-functionalized graphene decorated with Pt nanoparticles and its application in photocatalytic hydrogen production," *Int. J. Hydrogen Energy* **37**, 4880–4888 (2012).
120. S. K. Pilli et al., "Light induced water oxidation on cobalt-phosphate (Co-Pi) catalyst modified semi-transparent, porous SiO<sub>2</sub>-BiVO<sub>4</sub> electrodes," *Phys. Chem. Chem. Phys.* **14**, 7032–7039 (2012).
121. D. K. Zhong et al., "Photo-assisted electrodeposition of cobalt-phosphate (Co-Pi) catalyst on hematite photoanodes for solar water oxidation," *Energy Environ. Sci.* **4**, 1759–1764 (2011).
122. J. Y. Zheng et al., "Preparation of  $\alpha$ -Fe<sub>2</sub>O<sub>3</sub> films by electrodeposition and photodeposition of Co-Pi on them to enhance their photoelectrochemical properties," *RSC Adv.* **5**, 36307–36314 (2015).
123. A. J. Esswein et al., "Highly active cobalt phosphate and borate based oxygen evolving catalysts operating in neutral and natural waters," *Energy Environ. Sci.* **4**, 499–504 (2011).
124. Y. Surendranath, M. Dinca, and D. G. Nocera, "Electrolyte-dependent electrosynthesis and activity of cobalt-based water oxidation catalysts," *J. Am. Chem. Soc.* **131**, 2615–2620 (2009).
125. M. W. Kanan, Y. Surendranath, and D. G. Nocera, "Cobalt-phosphate oxygen-evolving compound," *Chem. Soc. Rev.* **38**, 109–114 (2009).
126. M. W. Kanan and D. G. Nocera, "In situ formation of an oxygen-evolving catalyst in neutral water containing phosphate and Co<sup>2+</sup>," *Science* **321**, 1072–1075 (2008).
127. A. Indra et al., "Nickel as a co-catalyst for photocatalytic hydrogen evolution on graphitic-carbon nitride (sg-CN): what is the nature of the active species," *Chem. Commun.* **52**, 104–107 (2016).
128. Y. Xu and R. Xu, "Nickel-based cocatalysts for photocatalytic hydrogen production," *Appl. Surf. Sci.* **351**, 779–793 (2015).
129. M. Shen et al., "MoS<sub>2</sub> nanosheet/TiO<sub>2</sub> nanowire hybrid nanostructures for enhanced visible-light photocatalytic activities," *Chem. Commun.* **50**, 15447–15449 (2014).
130. Y. Hou et al., "Bioinspired molecular co-catalysts bonded to a silicon photocathode for solar hydrogen evolution," *Nat. Mater.* **10**, 434–438 (2011).
131. X. Morales et al., "Hydrogen evolution from a copper(I) oxide photocathode coated with an amorphous molybdenum sulphide catalyst," *Nat. Commun.* **5**, 3059 (2014).
132. X. Zong et al., "Enhancement of photocatalytic H<sub>2</sub> evolution on CdS by loading MoS<sub>2</sub> as cocatalyst under visible light irradiation," *J. Am. Chem. Soc.* **130**, 7176–7177 (2008).
133. R. Jiang et al., "Metal/semiconductor hybrid nanostructures for plasmon-enhanced applications," *Adv. Mater.* **26**, 5274–5309 (2014).
134. X. Zhang et al., "Plasmonic photocatalysis," *Rep. Prog. Phys.* **76**, 046401 (2013).
135. S. C. Warren and E. Thimsen, "Plasmonic solar water splitting," *Energy Environ. Sci.* **5**, 5133–5146 (2012).
136. C. G. Silva et al., "Influence of excitation wavelength (UV or visible light) on the photocatalytic activity of titania containing gold nanoparticles for the generation of hydrogen or oxygen from water," *J. Am. Chem. Soc.* **133**, 595–602 (2011).
137. M. K. Kumar et al., "Field effects in plasmonic photocatalyst by precise SiO<sub>2</sub> thickness control using atomic layer deposition," *ACS Catal.* **1**, 300–308 (2011).
138. W. Zhai et al., "Plasmon-driven selective oxidation of aromatic alcohols to aldehydes in water with recyclable Pt/TiO<sub>2</sub> nanocomposites," *Chem. Catal. Chem.* **3**, 127–130 (2011).
139. D. B. Ingram and S. Linic, "Water splitting on composite plasmonic-metal/semiconductor photoelectrodes: evidence for selective plasmon-induced formation of charge carriers near the semiconductor surface," *J. Am. Chem. Soc.* **133**(14), 5202–5205 (2011).



140. J. J. Chen et al., "Plasmonic photocatalyst for H<sub>2</sub> evolution in photocatalytic water splitting," *J. Phys. Chem. C* **115**, 210–216 (2011).
141. Z. Liu et al., "Plasmon resonant enhancement of photocatalytic water splitting under visible illumination," *Nano Lett.* **11**, 1111–1116 (2011).
142. S. Linic, P. Christopher, and D. B. Ingram, "Plasmonic-metal nanostructures for efficient conversion of solar to chemical energy," *Nat. Mater.* **10**, 911–921 (2011).
143. T. Butburee et al., "Step-wise controlled growth of metal at TiO<sub>2</sub> core-shells with plasmonic hot spots and their photocatalytic properties," *J. Mater. Chem. A* **2**, 12776–12784 (2014).
144. K. Cheng et al., "Plasmon-enhanced photocurrent generation in quantum dots-sensitized solar cells by coupling of gold nanocrystals," *Sci. Bull.* **60**, 541–548 (2015).
145. H. Chen, G. Liu, and L. Wang, "Switched photocurrent direction in Au/TiO<sub>2</sub> bilayer thin films," *Sci. Rep.* **5**, 10852 (2015).
146. J. Xiong et al., "Facile synthesis of highly efficient one-dimensional plasmonic photocatalysts through Ag at Cu<sub>2</sub>O core-shell heteronanowires," *ACS Appl. Mater. Interfaces* **6**, 15716–15725 (2014).
147. J. Li et al., "Plasmon-induced photonic and energy-transfer enhancement of solar water splitting by a hematite nanorod array," *Nat. Commun.* **4**, 2651 (2013).
148. X. Zhao et al., "Ag nanoparticles decorated CuO nanowire arrays for efficient plasmon enhanced photoelectrochemical water splitting," *Chem. Phys. Lett.* **609**, 59–64 (2014).
149. W. Fan et al., "In situ deposition of Ag-Ag<sub>2</sub>S hybrid nanoparticles onto TiO<sub>2</sub> nanotube arrays towards fabrication of photoelectrodes with high visible light photoelectrochemical properties," *Phys. Chem. Chem. Phys.* **16**, 676–680 (2014).
150. K. Chen et al., "Effect of Ag nanoparticle size on the photoelectrochemical properties of Ag decorated TiO<sub>2</sub> nanotube arrays," *J. Alloys Compd.* **554**, 72–79 (2013).
151. S. Y. Reece et al., "Wireless solar water splitting using silicon-based semiconductors and earth-abundant catalysts," *Science* **334**, 645–648 (2011).
152. D. V. Esposito et al., "H<sub>2</sub> evolution at Si-based metal-insulator–semiconductor photoelectrodes enhanced by inversion channel charge collection and H spillover," *Nat. Mater.* **12**, 562–568 (2013).
153. B. Seger et al., "Using TiO<sub>2</sub> as a conductive protective layer for photocathodic H<sub>2</sub> evolution," *J. Am. Chem. Soc.* **135**, 1057–1064 (2013).
154. S. Licht et al., "Efficient solar water splitting, exemplified by RuO<sub>2</sub>-catalyzed AlGaAs/Si photoelectrolysis," *J. Phys. Chem. B* **104**, 8920–8924 (2000).
155. F. F. Abdi et al., "Efficient solar water splitting by enhanced charge separation in a bismuth vanadate-silicon tandem photoelectrode," *Nat. Commun.* **4**, 2195 (2013).
156. Y. Li et al., "Cobalt phosphate-modified barium-doped tantalum nitride nanorod photoanode with 1.5% solar energy conversion efficiency," *Nat. Commun.* **4**, 2566 (2013).
157. "Hydrogen evolution from Pt/Ru-coated p-type WSe<sub>2</sub> photocathodes," *J. Am. Chem. Soc.* **135**, 223–231 (2013).
158. X. Wang et al., "Silicon/hematite core/shell nanowire array decorated with gold nanoparticles for unbiased solar water oxidation," *Nano Lett.* **14**, 18–23 (2014).
159. J. Y. Kim et al., "Single-crystalline, wormlike hematite photoanodes for efficient solar water splitting," *Sci. Rep.* **3**, 2681 (2013).
160. A. Paracchino et al., "Highly active oxide photocathode for photoelectrochemical water reduction," *Nat. Mater.* **10**, 456–461 (2011).
161. P. Borno et al., "A bismuth vanadate-cuprous oxide tandem cell for overall solar water splitting," *J. Phys. Chem. C* **118**, 16959–16966 (2014).
162. Z. Zhang et al., "Carbon-layer-protected cuprous oxide nanowire arrays for efficient water reduction," *ACS Nano* **7**, 1709–1717 (2013).
163. M. Moriya et al., "Stable hydrogen evolution from CdS-modified CuGaSe<sub>2</sub> photoelectrode under visible-light irradiation," *J. Am. Chem. Soc.* **135**, 3733–3735 (2013).
164. L. Zhang et al., "Hydrogen evolution from water using Ag<sub>x</sub>Cu<sub>1-x</sub>GaSe<sub>2</sub> photocathodes under visible light," *Phys. Chem. Chem. Phys.* **16**, 6167–6174 (2014).



165. J. Luo et al., "Water photolysis at 12.3% efficiency via perovskite photovoltaics and Earth-abundant catalysts," *Science* **345**, 1593–1596 (2014).
166. P. Da et al., "High-performance perovskite photoanode enabled by Ni passivation and catalysis," *Nano Lett.* **15**, 3452–3457 (2015).
167. J. K. Kim et al., "Synthesis of transparent mesoporous tungsten trioxide films with enhanced photoelectrochemical response: application to unassisted solar water splitting," *Energy Environ. Sci.* **4**, 1465–1470 (2011).
168. J. Brilliet et al., "Highly efficient water splitting by a dual-absorber tandem cell," *Nat. Photonics* **6**, 824–828 (2012).
169. X. Shi et al., "Unassisted photoelectrochemical water splitting beyond 5.7% solar-to-hydrogen conversion efficiency by a wireless monolithic photoanode/dye-sensitised solar cell tandem device," *Nano Energy* **13**, 182–191 (2015).
170. S. Ryu et al., "Voltage output of efficient perovskite solar cells with high open-circuit voltage and fill factor," *Energy Environ. Sci.* **7**, 2614–2618 (2014).
171. J. H. Kim et al., "Wireless solar water splitting device with robust cobalt-catalyzed, dual-doped BiVO<sub>4</sub> photoanode and perovskite solar cell in tandem: a dual absorber artificial leaf," *ACS Nano* **9**, 11820–11829 (2015).
172. C. Ding et al., "Solar-to-hydrogen efficiency exceeding 2.5% achieved for overall water splitting with an all earth-abundant dual-photoelectrode," *Phys. Chem. Chem. Phys.* **16**, 15608–15614 (2014).
173. J.-W. Jang et al., "Enabling unassisted solar water splitting by iron oxide and silicon," *Nat. Commun.* **6**, 7447 (2015).
174. G. K. Mor et al., "p-type Cu-Ti-O nanotube arrays and their use in self-biased heterojunction photoelectrochemical diodes for hydrogen generation," *Nano Lett.* **8**, 1906–1911 (2008).
175. S. Khan, M. Frites, and W. B. Ingler, "Single chip standalone water splitting photoelectrochemical cell," *J. Technol. Innovation Renewable Energy* **3**, 6–11 (2014).
176. M. R. Shaner et al., "Si/TiO<sub>2</sub> tandem-junction microwire arrays for unassisted solar-driven water splitting," *J. Electrochem. Soc.* **163**, H261–H264 (2016).
177. P. Yang and J. M. Tarascon, "Towards systems materials engineering," *Nat. Mater.* **11**, 560–563 (2012).
178. H. S. Park et al., "Unbiased photoelectrochemical water splitting in Z-scheme device using W/Mo-doped BiVO<sub>4</sub> and Zn<sub>x</sub>Cd<sub>1-x</sub>Se," *Chem. Phys. Chem.* **14**, 2277–2287 (2013).
179. H. B. Yang et al., "Stable quantum dot photoelectrolysis cell for unassisted visible light solar water splitting," *ACS Nano* **8**, 10403–10413 (2014).
180. B. AlOtaibi et al., "A metal-nitride nanowire dual-photoelectrode device for unassisted solar-to-hydrogen conversion under parallel illumination," *Nano Lett.* **15**, 6821–6828 (2015).

**Piangjai Peerakiatkhajohn** received her MSc degree from the Joint Graduate School of Energy and Environment (JGSEE), King Mongkut's University of Technology Thonburi in 2011. Currently, she is a PhD student under the supervision of Prof. Lianzhou Wang at School of Chemical Engineering, The University of Queensland (UQ), Australia. Her research interest focuses on the design and development of novel photoelectrochemical system for efficient solar energy conversion.

**Jung-Ho Yun** received his PhD degree in chemical engineering from the University of New South Wales in 2012. Before his PhD, he worked at NANOPAC, Korea, for energy/environmental applications using functional nanomaterials between 2003 and 2007. Currently, he is working as a postdoctoral research fellow in Prof. Lianzhou Wang's Group, The University of Queensland. His research focuses on novel nanostructured photoelectrodes for photoelectrochemical system and solar cells.

**Songcan Wang** received his BEng. (2011) and MEng. (2014) from the Central South University (CSU), China. Currently, he is a PhD student under the supervision of Prof. Lianzhou Wang at School of Chemical Engineering, The University of Queensland (UQ), Australia. His research

interests are mainly focused on the design and development of high performance photoanodes for photoelectrochemical energy storage and conversion.

**Lianzhou Wang** is currently a professor in the School of Chemical Engineering and director of the Nanomaterials Centre, the University of Queensland (UQ), Australia. He received his PhD degree from Shanghai Institute of Ceramics, Chinese Academy of Sciences, in 1999. Before joining UQ in 2004, he worked at two national institutes (NIMS and AIST) of Japan for 5 years. His research interests include the design and application of semiconducting nanomaterials in renewable energy conversion/storage systems, including photocatalysts and low-cost solar cells.